Isothermal calorimetric study on the heat evolution and the apparent activation energy of alkali-activated slag/fly ash pastes

Zhang, S.; Zuo, Y.; Li, Z.; Ye, G.

Publication date
2019

Document Version
Accepted author manuscript

Published in
The 2nd International Conference on Sustainable Building Materials

ICSBM 2019
2nd International Conference of Sustainable Building Materials
12-15 August, Eindhoven The Netherlands

Isothermal Calorimetric Study on Heat Evolution and Apparent Activation Energy of Alkali-activated Slag/Fly ash Pastes

Shizhe Zhang[1], Yibing Zuo[1], Zhenming Li[1], Guang Ye[1,*]

[1]Microlab, Section Materials and Environment, Faculty of Civil Engineering and Geosciences, Delft University of Technology, Stevinweg 1, 2628 CN, Delft, The Netherlands

[*]G.Ye@tudelft.nl

Key Words: Activation energy; alkali-activation; isothermal calorimetry; Slag; Fly ash

Abstract

Alkali-activated slag/fly ash (AASF) as an environmental-friendly binder system for construction materials has recently attracted great attention from both academic and industrial communities. Towards its wider engineering application, it is crucial to have a better understanding of the temperature induced effects by different curing regimes and the temperature sensitivity on the thermal properties of this system, for instance the apparent activation energy (E_a). However, the available information on E_a of AASF system is still quite limited.

The present study is aimed at investigating the role of alkaline activator chemistry on the reaction kinetics of AASF at early age. The binder is made of 50 wt.% blast furnace slag and 50 wt.% fly ash. Four alkaline activator silicate moduli (SiO_2/Na_2O ratio = 0.8, 1.0, 1.2 and 1.5) were used for the mixture preparation. The effect of activator modulus on the heat evolution was studied by performing isothermal calorimetry test up to 160 h at both 20°C and 40 °C. The cumulative heat release and ultimate total heat were studied through curve fitting using exponential model. Furthermore, the E_a of AASF pastes was determined using incremental methods and its variation over wide range of early age reaction was studied. It was found that the activator modulus evidently influences the heat evolution of AASF. The cumulative heat release reached the maximum value at activator modulus of 1.0, followed by at 0.8, 1.2 and 1.5. This trend is inversely related to the changes of E_a of AASF mixtures. In addition, it was confirmed that the E_a of AASF was not only related to the chemistry of reactants but also reaction-stage dependent. Particularly it varied significantly at the very early age of reaction.

1 General introductions

Alkali-activated materials (AAMs), derived by the reaction of an alkali metal source (solid or dissolved) with a solid (alumino)silicate powder [1, 2], are considered as an environmental friendly binder and one of the best alternatives for ordinary Portland cement (OPC). These materials show comparable or even better performances and less energy consumption at the same time when compared to the traditional cementitious binders. Furthermore, concrete made of alkali-activated materials also provide added advantage regarding the greenhouse gas emission. It is reported that a CO_2 reduction up to 80% could be achieved compared to concrete made of OPC [3]. Up till now, the most intensively studied system of AAMs is based on blast furnace slag and class F fly ash. This is mainly due to their large quantity of annual production as well as their relatively stable chemical composition. Previous studies on AASF have focused on microstructure development, nature of reaction products and mechanical properties [4-6]. However, few studies have paid attention to the heat evolution related properties, for instance, the apparent activation energy (E_a) of AASF. As an important parameter for engineering predictions and applications of AASF under different temperature curing regime, the knowledge of the E_a of AASF binder system is crucial.

Compared to that of traditional cementitious systems, the data concerning the E_a of AASF is currently still scarce. Most previous results were related to alkali-activated slag (AAS). For instance, Fernandez et al [7] determined E_a to be 57.6 kJ/mol in AAS system activated by sodium hydroxide and sodium silicate. Zhou [8] studied the kinetics of hydration of AAS and the E_a was determined to be 53.63 kJ/mol. Only one work related to the E_a in AASF was found [9] and the value calculated was 53.1 kJ/mol.

Therefore, this work aims to further investigate the influence of mixture parameters, especially the modulus, on the heat evolution and to determine the apparent activation energy of AASF systems by isothermal calorimetry testing.

2 Experimental program

2.1 Materials and mix design

The solid precursors used in this study were ground granulated blast furnace slag and Class F fly ash according to ASTM 618. Material density is 2890 kg/m^3 for slag and 2440 kg/m^3 for fly ash. The d50 particle size is 17.88 μm for slag and 33.19 μm for fly ash. The chemical compositions deduced from X-ray Fluorescence along with other properties of the precursors (including LOI at 950 °C and fineness passing 45 μm) are shown in Table 1.

Table 1. Chemical compositions and properties of raw materials

Oxide (wt %)	SiO_2	Al_2O_3	Fe_2O_3	CaO	MgO	SO_3	Na_2O	K_2O	LOI	Fineness, % passing 45μm
Slag	32.91	11.84	0.46	40.96	9.23	1.60	-	0.33	1.15	95
Fly ash	52.90	26.96	6.60	4.36	1.50	0.73	0.17	-	3.37	81

As reported previously by the authors [10], the major crystalline phases in fly ash are quartz, mullite and hematite, while the blast furnace slag contains mainly amorphous phases. The reactivity of slag could be indicatd by its abundant amorphous content (over 98%). On the other hand, the reactivity of fly ash is reflected by its reactive silica content of 43.04% and reactive alumina content of 15.51%.

To study the heat evolution of AASF, four levels of alkaline activator silicate moduli (ratio of SiO_2 wt.%/Na_2O wt.%) were considered for preparation of AASF pastes with fixed binder combination of 50 wt.% blast furnace slag and 50 wt.% fly ash. The detailed mixture designs are shown in Table 2. Na_2O wt.% content in alkaline activator (with respect to total binder mass) was kept constant to be 4%. In addition, the water to binder (w/b) ratio was chosen to be 0.32 to maintain adequate workability for all the paste mixtures. The mixtures were named M0.8, M1.0, M1.2 and M1.5 accordingly, with the number representing the activator modulus.

Table 2 Mixture design of AASF

Mixture	Slag (wt.%)	Fly ash (wt.%)	w/b ratio	Na_2O (wt.%)	Activator modulus
M0.8	50	50	0.32	4.0	0.8
M1.0					1.0
M1.2					1.2
M1.5					1.5

The alkaline activator was prepared by dissolving NaOH pellets (analytical grade, purity≥98%) and sodium silicate (Na_2O: 8.25 wt.%, SiO_2: 27.50 wt.%) in distilled water. The activator was cooled down to room temperature prior to mixture preparation.

2.2 Isothermal calorimetry

Isothermal calorimetry was conducted using a TAM-Air-314 isothermal conduction calorimeter. Calibration of the heat flow channels was carried out prior to measurements. The solid precursors were firstly hand mixed for 5 min. Afterwards, the alkaline activator solution was added and the batches were mixed for additional 2 min using a head-mixer with speed of 1600 rpm. Approximately 5 g of freshly mixed paste was introduced into a small glass ampoule and was immediately loaded into the heat flow channels along with the reference ampoule. Two replicates for each mixture were measured. Heat release was recorded for a period of 160 h. For the tests carried out at 40 °C, the solid precursors, alkaline activator and reference

ampoules were stored in 40 °C oven before the tests. Extra caution has been paid to minimize the decrease of temperature during mixing and transportation.

2.3 Ultimate total heat and global reaction degree through curve fitting

The ultimate total heat and the global reaction degree of AASF are calculated using cumulative heat release data by the aid of curve fitting using exponential model shown in Equation 1.

$$\mathrm{Q(t)} = Q_{max} \exp\left(\frac{-\tau}{t}\right)^{\beta} \quad (1)$$

where Q_{max} corresponds to the ultimate total heat at completion of reaction; τ and β are parameters associated with time and shape in the exponential model. This model has been proven somewhat adequate for Q_{max} prediction and has been previously used in alkali-activated systems [11, 12], especially when the data before the induction period is neglected. Through curve fitting, Q_{max} of all mixtures at 20 °C and 40 °C were determined. Finally, the reaction degree α(t) was calculated by Equation 6

$$\alpha(\mathrm{t}) = \frac{\mathrm{Q(t)}}{Q_{max}} \quad (2)$$

where α(t) was determined for all AASF mixtures reacted under 20 °C and 40 °C for later calculation of apparent activation energy using incremental method.

2.4 Apparent activation energy determination

Arrhenius's theory as shown in Equation 3 has been proven to be an effective tool to study the temperature related effects and combined rate sensitivity of hydration reactions in cementitious systems. The Arrhenius equation is written as:

$$\mathrm{k(T)} = \mathrm{A}\exp(\frac{-E_a}{RT}) \quad (3)$$

where k is the temperature sensitivity rate constant, T is the absolute temperature (K). A is a constant (pre-exponential factor that varies for different chemical reaction), E_a is the activation energy (kJ/mol), R is the universal gas constant (J/(mol·K)).

Arrhenius equation could be rewritten using two sets of rates constants at different temperature:

$$\mathrm{k}(T_1) = \mathrm{k}(T_2)\exp\left[\frac{-E_a}{RT}\,(\frac{1}{T_1} - \frac{1}{T_2})\right] \quad (4)$$

This study used the incremental method or 'rates' method to determine the apparent activation energy E_a of AASF , which has been previously used for OPC pastes [13, 14]. Assuming the calorimeter is calibrated properly, the rate constant k equals to the power of heat flow measured for a given reaction degree α and reaction temperature T:

$$\mathrm{k(T)} = \mathrm{P}(\alpha, \mathrm{T}) \quad (5)$$

Therefore, in order to calculate E_a, two sets of heat flow data were used which enables calculation of E_a as a function of reaction degree α continuously.

$$E_a = R\left[\frac{T_1\,T_2}{T_1 - T_2}\,ln\left(\frac{P\,{}^{T_1}_{\alpha_0}}{P\,{}^{T_2}_{\alpha_0}}\right)\right] \quad (6)$$

It is worth noting that a huge simplification is made here to use E_a for the entire alkali activation and geopolymerization processes. Evidently, E_a is also sensitive to different reaction stages as the microstructure changes with elapse of time. However, considering the great difficulties to distinguish the different individual reactions within geopolymerization, E_a acquired in this way can still give further insights on temperature dependent reaction kinetics of the global reaction.

3 Results and discussions

3.1 Heat evolution and reaction degree

The heat flow curves of mixture M0.8-M1.5 under the temperature of 20 °C and 40 °C are shown in Figure 1. In general, the heat flow curve is characterized by two calorimetric peaks: the first peak is due to the wetting and dissolution of precursors particles and the second broader peak corresponds to the formation of reaction products. Compared to the heat flow at 20 °C, an evident increase of heat flow intensity could be found at 40 °C. In addition, the intensity and the time of appearance of the second peak are positively correlated and both of them change with increasing activator modulus. More specifically, with increasing activator modulus, both the intensity and time of appearance of the second peak first increase and then decline after reaching the maximum when activator modulus is 1.2. This trend indicates activator modulus has a significant influence over the early age reaction kinetics of AASF. It is commonly acknowledged that the early age reaction of AASF is dominated by two processes, i.e. the dissolution of Ca, Si, Al species from the solid precursor and Si oligomer dissociation presented in alkaline activator, and the geopolymerization of available species to form various reaction products. Previous studies by ^{29}Si NMR and FTIR proved that higher amount of silica species with low polymerization degree (monomers) is favoured at lower activator modulus [15, 16], A lower polymerization degree of silica species can promote the gel formation. However, by lowering the activator modulus, the total amount of available species within alkaline activator is also reduced, which might have negative impact over the very early geopolymerization process.

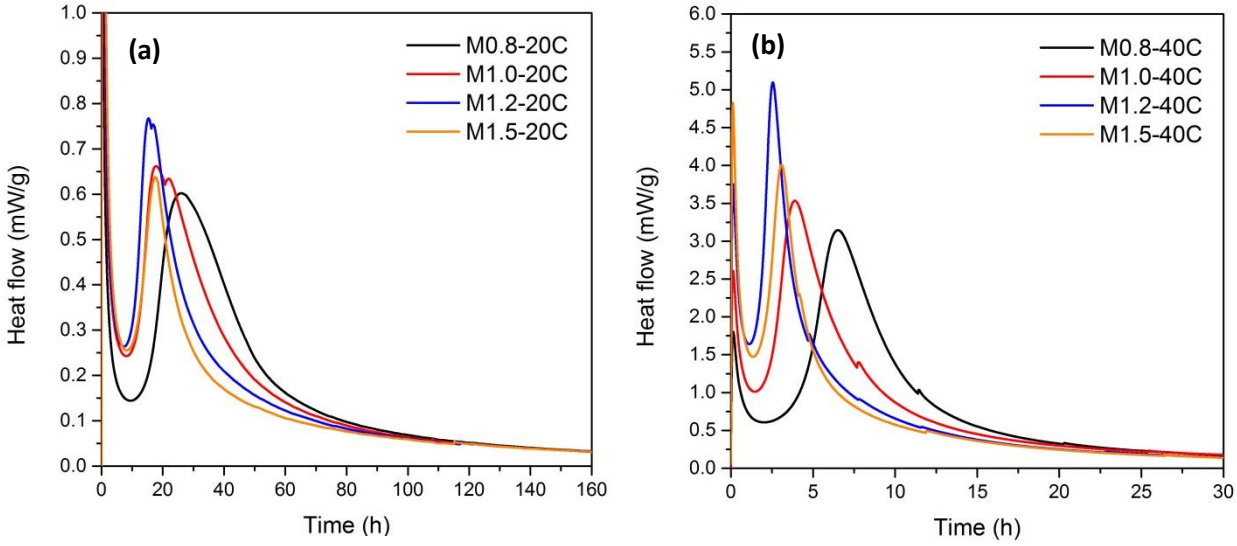

Figure 1 Heat flow of AASF mixtures at different temperature: (a) 20°C; (b) 40°C

The experimental data and corresponding curve fitting using exponential model were presented in Figure 2 (a) and (b). For the calculation of cumulative reaction heat, it is worth noting that the initial data related to the heat flow of first peak was not taken into consideration, which is in accord with previous studies [7, 17, 18]. The reason is to avoid the testing error induced during the mixing and transferring of the AASF mixtures.

As expected, the cumulative heat for AASF at 40 °C were evidently higher than that at 20 °C due to the facilitating effect on reaction rate induced by a higher temperature. At 160h, M1.0 has the highest cumulative heat release followed by M0.8, M1.2 and M1.5. This trend is not consistent with the trend of the heat flow of the main reaction peak, which reached maximum when activator modulus is 1.2. Therefore, it seems that a faster early age reaction is neither necessary nor sufficient for a higher reaction cumulative heat of AASF. In this study, the higher cumulative heat release of certain activator modulus could be related to the early age dissolution of species and the following-up geopolymerization process. With increasing activator modulus, the pH of alkaline activator drops [16]. Although in this way the early age dissolution is slowed

down, higher activator modulus increases the total amount of available species for geopolymerization in the liquids. Hence, an optimum activating conditions for overall reaction would exist which is favoured by its higher ultimate heat release and higher amount of main reaction products.

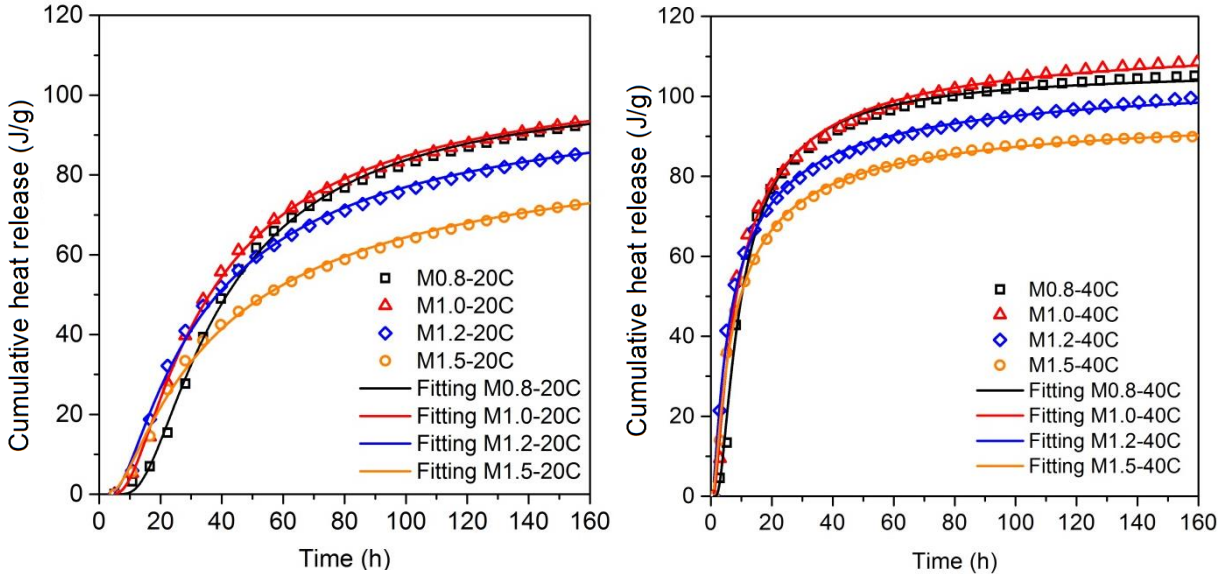

Figure 2 Cumulative heat release of AASF mixtures and curve fitting using the exponential model: (a) 20°C; (b) 40°C

The fitted parameters of exponential model for Q_{max} are presented in Table 3. As could be seen in Table 3, the accuracy of fitting (Adjusted R-Square) is rather satisfactory, implying the effectiveness of using exponential model for cumulative heat fitting in AASF. In addition, the Q_{max} obtained exhibits identical trend with increasing activator modulus when comparing with corresponding cumulative heat release Q_{160h} of AASF up to 160h.

Table 3 Fitted parameters of exponential model for cumulative heat release

Mixture		**M0.8**		**M1.0**		**M1.2**		**M1.5**	
		20 °C	**40 °C**	**20 °C**	**40 °C**	**20 °C**	**40 °C**	**20 °C**	**40 °C**
Cumulative heat at 160h	Q_{160h}	92.8	105.1	93.6	108.5	85.7	99.8	73.1	89.9
Fitting parameters	Q_{max}	103.55	106.65	107.46	114.95	103.30	106.80	94.47	97.24
	τ	33.33	8.03	28.49	6.73	27.53	5.27	31.70	5.79
	β	1.41	1.22	1.14	0.86	0.95	0.73	0.84	0.78
Adjusted R-Square	r^2	0.998	0.996	0.999	0.996	0.998	0.996	0.997	0.997

3.2 Apparent activation energy E_a

The apparent activation energy E_a of AASF with various activator modulus was determined using incremental method (Equation 6) and the evolution of E_a as a function of reaction degree of AASF is shown in Figure 3. In general, E_a varies largely at the early age of the reaction for all mixtures. It is observed that E_a firstly increase to a maximum value and then declines until reaching a relative stable value after reaction degree of 50%.

It is believed that this large variation is associated with the nature of chemical reaction, in which dissolution is dominant in early age reactions. In later main reaction stage, E_a becomes stable since the reaction is gradually moving into a diffusion-controlled stage. Similar trend of E_a development as function of reaction degree (or cumulative heat release) was also reported in previous works in cementitious system [19] and alkali-activated system [9]. Therefore, E_a is deduced taking the average value from the stabilized part from

reaction degree 50% to 80%. In this study. E_a of AASF activated by sodium hydroxide and sodium silicate changes from 24.6 to 46.4 kJ/mol with the variation of activator modulus. The value of E_a for M0.8, M1.0, M1.2 and M1.5 are 32.0±1.7, 24.6±2.1, 39.2±2.4 and 46.4±2.2 kJ/mol, respectively. The trend of E_a with increasing activator modulus, is clearly inversely related with the trend of Q_{160h}, which is considered reasonable since lower apparent activation energy implies a lower energy barrier for geopolymerization. At a certain temperature, the reaction rate at of AASF was in a way facilitated and yielded higher amount of reaction heat at 160h.

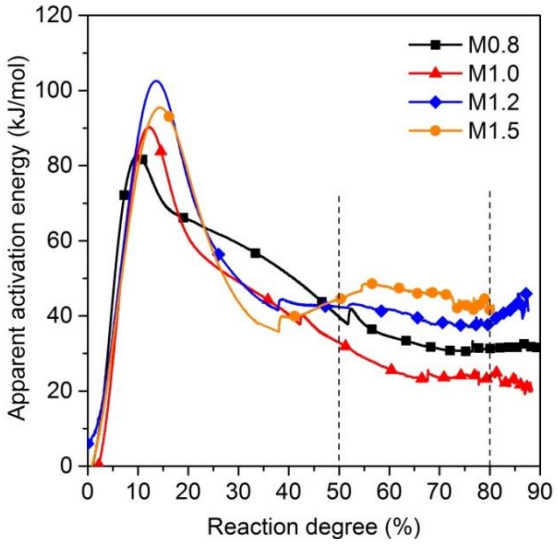

Figure 3 Apparent activation energy E_a as a function of reaction degree

According to previous studies of E_a of alkali-activated systems, comparison of related results is made and is shown in Table 4. It could be found that E_a determined in AASF is in general lower than those determined in AAS systems and close to the value determined in AASF systems. However, it is crucial to notice that by changing activator modulus, more silica is introduced into the system and the global chemical reaction is already changed. E_a as one of its reflections, therefore, cannot be directly used to compare the chemical nature and ultimate total heat release of different AASF systems.

Table 4 Apparent activation energy Ea for different alkali-activated systems

E_a	Solid precursor	Activator (Liquids)	Reference
57.6	GGBS	$NaOH+Na_2SiO_3$ (Na_2O% = 4%)	Fernandez et al [7].
53.6	GGBS	$NaOH+Na_2SiO_3$	Zhou et al [8].
48.2 ± 2.9	GGBS	9M NaOH	Sun & Vollpracht [20]
48.2 ± 5.9	80%GGBS+20%FA	8M $NaOH+Na_2SiO_3$	Joseph et al [9].
24.6 ~ 46.4	50%GGBS+50%FA	$NaOH+Na_2SiO_3$ (Na_2O% = 4%)	Present study

4 Conclusions

The present study is aimed at investigating the role of alkaline activator chemistry and temperature on the early age reaction kinetics of AASF made of 50 wt.% blast furnace slag and 50 wt.% fly ash. The effect of activator modulus on the heat evolution and cumulative reaction heat release was studied. Additionally, the apparent activation energy was determined using the incremental method and its variation over wide range of early age reaction was studied.

It was found that the activator modulus evidently influences the heat evolution of AASF. The cumulative heat release at 160h reached the maximum value at activator modulus of 1.0, followed by at 0.8, 1.2 and 1.5. This trend is inversely related to the changes of the apparent activation energy E_a of AASF mixtures. Disagreement of the trend of early age heat flow and that of cumulative reaction heat implies that a faster early age reaction does not necessarily result in a higher ultimate total heat of AASF. The calculated E_a varies from 24.6 to 46.4 kJ/mol, which is in generally close to the values reported for GGBS based alkali activated

systems. Furthermore, this study confirmed that the apparent activation energy of AASF was not only related to the chemistry of reactants but also reaction-stage dependent. Particularly it varied significantly at the very early age of reaction.

5 Acknowledgements

This research is carried out in Microlab, Delft University of Technology and supported by the Netherlands Organisation for Scientific Research (NWO), Grant No.729.001.013 and National Natural Science Foundation of China (NSFC), Grant No. 5151101050. Additionally, the second and third author would like to thank the financial support from China Scholarship Council (CSC).

6 References

1. Shi, C., D. Roy, and P. Krivenko, *Alkali-activated cements and concretes*. 2006: CRC press.

2. Davidovits, J., *Geopolymers*. Journal of Thermal Analysis and Calorimetry, 1991. **37**(8): p. 1633-1656.

3. Duxson, P., et al., *The role of inorganic polymer technology in the development of 'green concrete'*. Cement and Concrete Research, 2007. **37**(12): p. 1590-1597.

4. Ismail, I., et al., *Modification of phase evolution in alkali-activated blast furnace slag by the incorporation of fly ash*. Cement and Concrete Composites, 2014. **45**: p. 125-135.

5. Puertas, F. and A. Fernández-Jiménez, *Mineralogical and microstructural characterisation of alkali-activated fly ash/slag pastes*. Cement and Concrete composites, 2003. **25**(3): p. 287-292.

6. Lee, N.K. and H.K. Lee, *Reactivity and reaction products of alkali-activated, fly ash/slag paste*. Construction and Building Materials, 2015. **81**: p. 303-312.

7. Fernández-Jiménez, A. and F. Puertas, *Alkali-activated slag cements: kinetic studies*. Cement and concrete research, 1997. **27**(3): p. 359-368.

8. Huanhai, Z., et al., *Kinetic study on hydration of alkali-activated slag*. Cement and Concrete Research, 1993. **23**(6): p. 1253-1258.

9. Joseph, S., S. Uppalapati, and O. Cizer, *Instantaneous activation energy of alkali activated materials*. RILEM Technical Letters, 2018. **3**: p. 121-123.

10. Zhang, S., et al., *Waste glass as partial mineral precursor in alkali-activated slag/fly ash system*. Cement and Concrete Research, 2017. **102**: p. 29-40.

11. Chithiraputhiran, S. and N. Neithalath, *Isothermal reaction kinetics and temperature dependence of alkali activation of slag, fly ash and their blends*. Construction and Building Materials, 2013. **45**(0): p. 233-242.

12. Ravikumar, D. and N. Neithalath, *Reaction kinetics in sodium silicate powder and liquid activated slag binders evaluated using isothermal calorimetry*. Thermochimica Acta, 2012. **546**(0): p. 32-43.

13. Poole, J.L., et al., *Methods for calculating activation energy for Portland cement*. ACI Materials Journal, 2007. **104**(1): p. 303-311.

14. Broda, M., E. Wirquin, and B. Duthoit, *Conception of an isothermal calorimeter for concrete—Determination of the apparent activation energy*. Materials and Structures, 2002. **35**(7): p. 389-394.

15. Criado, M., et al., *Effect of the SiO_2/Na_2O ratio on the alkali activation of fly ash. Part II: ^{29}Si MAS-NMR Survey*. Microporous and Mesoporous Materials, 2008. **109**(1): p. 525-534.

16. Jansson, H., D. Bernin, and K. Ramser, *Silicate species of water glass and insights for alkali-activated green cement*. Aip Advances, 2015. **5**(6): p. 067167.

17. Fernández-Jiménez, A., F. Puertas, and A. Arteaga, *Determination of kinetic equations of alkaline activation of blast furnace slag by means of calorimetric data.* Journal of thermal analysis and calorimetry, 1998. **52**(3): p. 945-955.

18. Carette, J. and S. Staquet, *Monitoring and modelling the early age and hardening behaviour of eco-concrete through continuous non-destructive measurements: Part I. Hydration and apparent activation energy.* Cement and Concrete Composites, 2016. **73**: p. 10-18.

19. Kada-Benameur, H., E. Wirquin, and B. Duthoit, *Determination of apparent activation energy of concrete by isothermal calorimetry.* Cement and concrete research, 2000. **30**(2): p. 301-305.

20. Sun, Z. and A. Vollpracht, *Isothermal calorimetry and in-situ XRD study of the NaOH activated fly ash, metakaolin and slag.* Cement and Concrete Research, 2018. **103**: p. 110-122.